Multimode interference wavelength multi/demultiplexer for 1310 and 1550 nm operation based on BCB 4024-40 photodefinable polymer

M.H. Ibrahim [a,*], Shuh-Ying Lee [b], Mee-Koy Chin [b],
N. Mohd Kassim [a], A.B. Mohammad [a]

[a] *Photonics Technology Centre, Faculty of Electrical Engineering, Universiti Teknologi Malaysia, 81310 Johor, Malaysia*
[b] *Photonics Research Centre, School of Electrical and Electronic Engineering, Nanyang Technological University, Singapore*

Abstract

A 1310 and 1550 nm coarse wavelength multi/demultiplexer based on benzocyclobutene (BCB 4024-40) polymer is demonstrated for the first time. The device is designed based on a combination of general interference and paired interference mechanisms of multimode interference (MMI). It is fabricated on BK7 glass substrate with a thin layer of SiO_2 as cover. A cost effective chemical etching technique is used in the fabrication process to take advantage of the photosensitive nature of the polymer. The device length was significantly reduced by adopting the restricted multimode interference scheme, lower beat length ratio and cascaded MMI couplers. The measured crosstalk at 1310 nm was 14.4 dB and at 1550 nm was 20.6 dB. The measured insertion loss is around 3.2–3.5 dB for both ports.
© 2007 Elsevier B.V. All rights reserved.

1. Introduction

Wavelength splitting (demultiplexing) and combining (multiplexing) are important functions in many optical applications. An important example is fiber-to-the-home (FTTH) application where 1550 and 1310 nm wavelengths may be used to carry data/voice and video, respectively [1]. Since the wavelengths are spaced far apart, a very coarse wavelength division (de)multiplexer, or CWDM filter for short, would be needed to separate or combine the wavelengths. A bidirectional and compact filter that can be integrated with transceivers is desirable as it would facilitate the development of low-cost terminal units for the home. Such a filter could be realized using a multi-mode interferometer (MMI) coupler. Compared to other methods such as Y branch [2], Mach-Zender interferometer [3], and directional couplers [4], MMI couplers are considered superior, as they are quite easy to design and fabricate, and can also have broad optical bandwidth, low crosstalk, and small polarization dependence [5].

Various material have been applied in the design and realization of the MMI based optical devices which include silica [7,8], silicon [6], III–V semiconductor materials [9] and polymer [10]. Of this, polymeric materials are particularly attractive in integrated optics because of their ability to be processed rapidly, cost-effectively, and with high yields [11]. Classes of polymers used in integrated optics include acrylates, polyimides, polycarbonates and olefin (e.g., cyclobutene). Benzocyclobutene (BCB 4024-40), a product of Dow™, is a photodefinable polymer and is commonly used for board-level interconnects. Due to its low cost and low loss characteristics [12], it is a suitable candidate for optical device applications.

---

* Corresponding author. Tel.: +60 75535302; fax: +60 75566272.
 E-mail address: hanif@fke.utm.my (M.H. Ibrahim).

Most of the reports on the development of MMI based CWDM filter for coarse 1310 and 1550 nm wavelengths are focused on the device design and modeling, such as by Lin and Lee [13] on SiON–SiO$_2$ ridge waveguide, Chuang et al. [7] on SiON–SiO$_2$ ridge waveguide, and Tsao et al. [14] on SOI substrate. The only demonstration of MMI- based CWDM filter is reported by Paiam et al. [8] for coarse 980 and 1550 nm demultiplexing operation, using SiON–SiO$_2$ rib waveguide system. Based on our extensive review, no such work based on polymeric material has been reported for demultiplexing 1310 and 1550 nm, which indicates the originality of this work.

In this paper, we report a new design of MMI multi/demultiplexer for 1310 and 1550 nm based on BCB 4024-40 polymer. The waveguide is fabricated on BK7 glass substrate and is covered with a thin layer of SiO$_2$. A chemical etching technique is used in the fabrication process to take advantage of the photosensitive nature of the polymer. The use of low-cost process in combination with the low-cost materials makes this a potentially viable device for low-cost manufacturing.

In the following section we discuss some unique features in our design of the MMI. Due to wavelength insensitivity of the MMI effect, the device is relatively long for separating the 1310 and 1550 nm wavelengths. To minimize this length we use the restricted-interference scheme and design the MMI dimensions to minimize the beat length ratio. In Sections 3 and 4, we present the fabrication and test results.

2. Device principle and design

MMI couplers work on the principle of self imaging effect, a property of multimode waveguides by which an input field is reproduced in single or multiple images at periodic intervals along the propagation direction of the guide [6]. The lateral modes in the MMI section have different propagation constants. At certain distances, constructive interference between the modes produces single or multiple self images of the input field. Depending on the input field excitation condition, there are two possible types of interference. In *general interference* (GI), all modes are excited in the MMI section and constructive interference occurs at

$$z = p(3L_\pi) \tag{1}$$

where

$$L_\pi = \frac{\pi}{\beta_0 - \beta_1} \approx \frac{4nW_e^2}{3\lambda_0} \tag{2}$$

β_0 and β_1 are propagation constants of the fundamental and the first order lateral modes, respectively, λ_0 is a free-space wavelength, n is the effective index and W_e is the effective width of the multimode waveguide. When p is even, the output is a direct image of the input field and when p is odd it is a mirrored image. In the other scheme known as *restricted interference* (RI), certain modes are not excited and the resonant images occur at

$$z = p(L_\pi) \tag{3}$$

Note that this scheme allows the design to be three times shorter compared to GI. This type of multimode interference scheme can be realized by placing the input access waveguides at 1/3 or 2/3 of the MMI section width [15].

To separate two wavelengths such that λ_1 is in one output and λ_2 is in the other output ($\lambda_1 < \lambda_2$), the condition in the RI scheme is given by

$$L_d = pL_{\pi,\lambda_1} = (p + q)L_{\pi,\lambda_2} \tag{4}$$

where p is a positive integer, q is an odd integer, and L_π, λ_i is the beat length for wavelength λ_i. Note that L_π always decreases with increasing wavelength. In order to minimize device length, p and q should be as small as possible. Therefore, p and q are determined once the beat length ratio, $\frac{L_c(\lambda_1)}{L_c(\lambda_2)} = 1 + \frac{q}{p}$ is known.

The beat length ratio of $1 + \frac{q}{p}$ is determined by simulating the ratio of $\frac{L_{\pi,\lambda_1}}{L_{\pi,\lambda_2}}$, taking λ_1 as 1310 nm and λ_2 as 1550 nm, as a function of MMI width. The result for an MMI based on BCB 4024-40 is shown in Fig. 1. The polymer refractive index is taken to be 1.5556, based on measurement described in the following section. From the graph, we can see that the optimum beat length ratio is 1.1667 (i.e., $p = 6$ and $q = 1$) for an MMI width of $w = 23$ μm. $L_{\pi,1310}$ is 922.3 μm, hence the MMI length, L_d is 5534 μm.

With the MMI width used ($W_1 = 23$ μm), the output waveguide spacing is only 7.7 μm. To increase the spacing one could interpose S-curve waveguides. However, in our design we use an MMI cross coupler operating in each output waveguide to offset the outputs by about 13 μm, thereby increasing the separation to $W_3 = 34$ μm. These MMI couplers operate in the GI mode and have a width of $W_2 = 15$ μm. The schematic layout of the complete demultiplexer is shown in Fig. 2.
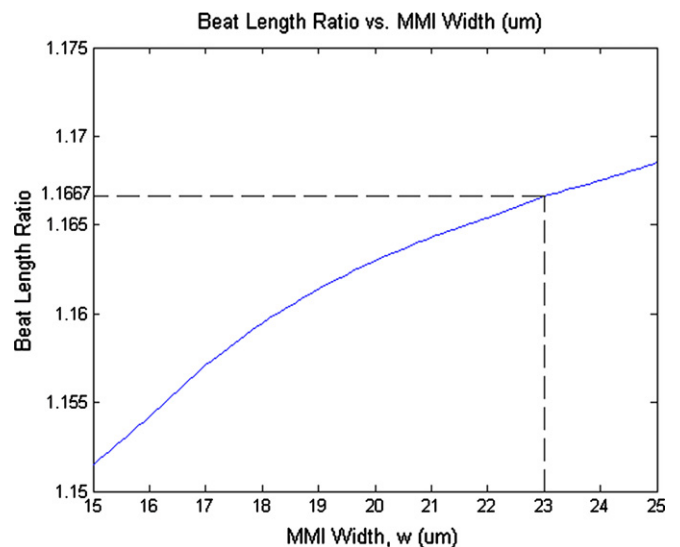

Fig. 1. Beat length ratio vs. MMI section width.
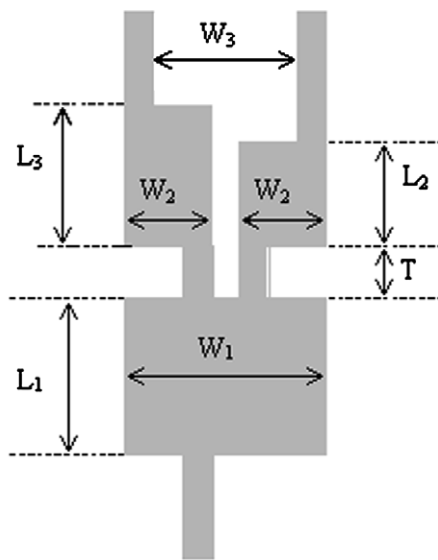
Fig. 2. Optical wavelength demultiplexer layout.

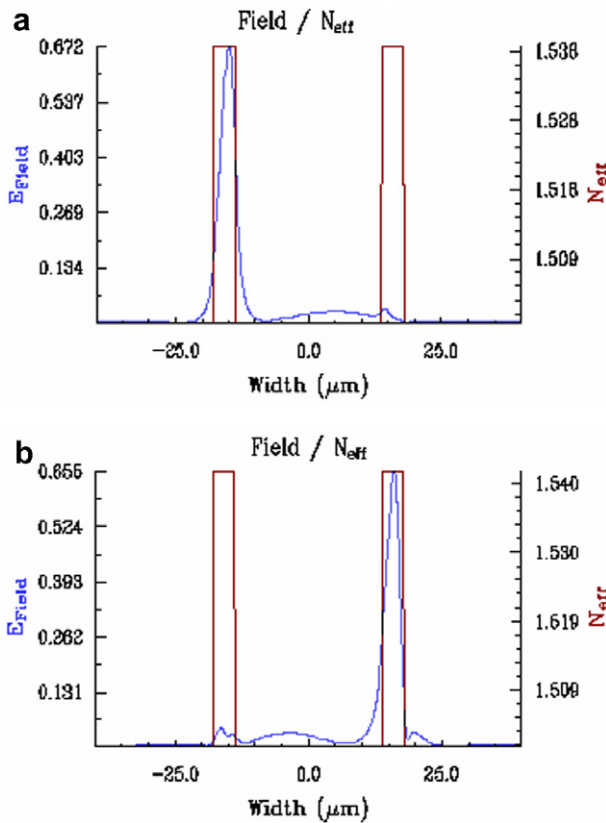L₂=1076 µm, L₃=1239 µm, T=200 µm

Fig. 3. 2D-BPM simulation intensity at (a) cross output for 1550 nm and (b) bar output for 1310 nm.

Light propagation through the MMI demultiplexer is modeled based on a combination of effective index method (EIM) and two-dimensional beam propagation method (2D-BPM). The simulation results are shown in Fig. 3.

3. Device fabrication and characterization

The starting material, BCB 4024-40, is a yellow amber liquid that is kept refrigerated at temperature below −15 °C and brought to room temperature before processing. Thin-film slab waveguides were fabricated on BK7 glass substrate by spin-coating at speeds ranging from 1500 to 6000 rpm. The slab waveguides were then measured for the average refractive index and film thickness using the prism coupling method [16,17]. To characterize the slab loss, the fiber probe method is applied in which the fiber is moved along the slab to measure the scattered power [18]. Fig. 4 shows the relation between the coating speed and the polymer slab thickness. The average refractive index obtained is 1.5556 for the TE polarization. The average value of slab loss is measured to be 1.01 dB/cm, showing the BCB 4024-40's ability in optical guiding application.

The process for the fabrication of channel waveguide using BCB 4024-40 is similar to the thin film multi-chip module process. According to our previous simulations [19], to produce a single-mode waveguide using this material structure, the core thickness required is about 4 µm. Hence, the coating speed of 3000 rpm and 4 µm of mask opening are chosen to realize a single-mode square waveguide structure.

In order to maintain good adhesion with the substrate layer, AP3000 adhesion promoter was spin coated on the substrates before polymer coating. After the polymer was spin coated, the film was heated on a hotplate for a specific time and temperature to drive out the residual solvent without film wrinkage. This is followed by the photolithography step using a dark field mask, as the BCB 4024-40 is a negative acting polymer. A mask aligner having I-line UV exposure at 365 nm wavelength was used to crosslink the exposed polymer region. The mask aligner power density was set to 3 mW/cm² and the exposure time was 20 s.
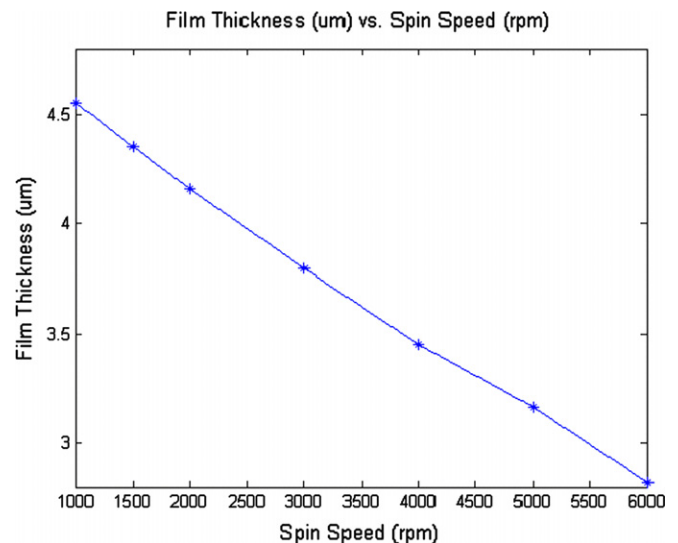

Fig. 4. Relation between polymer film thickness and coating speed.

After exposure, a pre-develop bake was carried out to increase the etching resistance and film adhesion to the substrate. The pre-develop bake temperatures were 10 °C lower than the pre-exposure bake. The chemical etching or developing process of BCB 4024-40 polymer requires the puddle development process. In this process, a DS2100 developer solvent was dispensed onto the sample surface. After 30 s of puddle time, the sample was rinsed for 10 s and spun at high speed to remove the developer solvent. To further dry the film and stabilize the side wall, the sample was baked on a hot plate immediately after developing. Finally, the sample was cured in a box oven at 250 °C to remove the residual solvents and harden the polymer. At the end of the process only the masked areas remain which form the waveguides. Note that neither photoresist nor RIE or plasma etching is necessary. However, the drawback of the chemical etching method is a reduced quality of the waveguide sidewall [12].

In order to reduce the refractive index difference between the waveguide core and the surrounding, a one-micron thick layer of SiO_2 was deposited on top of the

polymer using plasma enhanced chemical vapor deposition (PECVD) technique. The deposition process was carried out at 60 °C for 1 h. Finally, the waveguide sample was polished at the facets for optical coupling.

Images of the fabricated access waveguides and optical demultiplexers are shown in Fig. 5. The photo-patterned waveguides exhibit smooth polished end facets but significant sidewall roughness. The roughness is presumably due to the minor corrugations at the mask opening. It was also observed that the cross section of the waveguides is not perfectly rectangular due to the nature of the wet chemical etching process and the diffraction effects associated with the mask opening and film thickness. This agrees with other reported results based on chemical etching technique [20].

4. Results and discussion

For waveguide measurements, a single-mode fiber is used to couple 1550 nm TE laser source into the polished end facet of the access waveguide. The output is measured
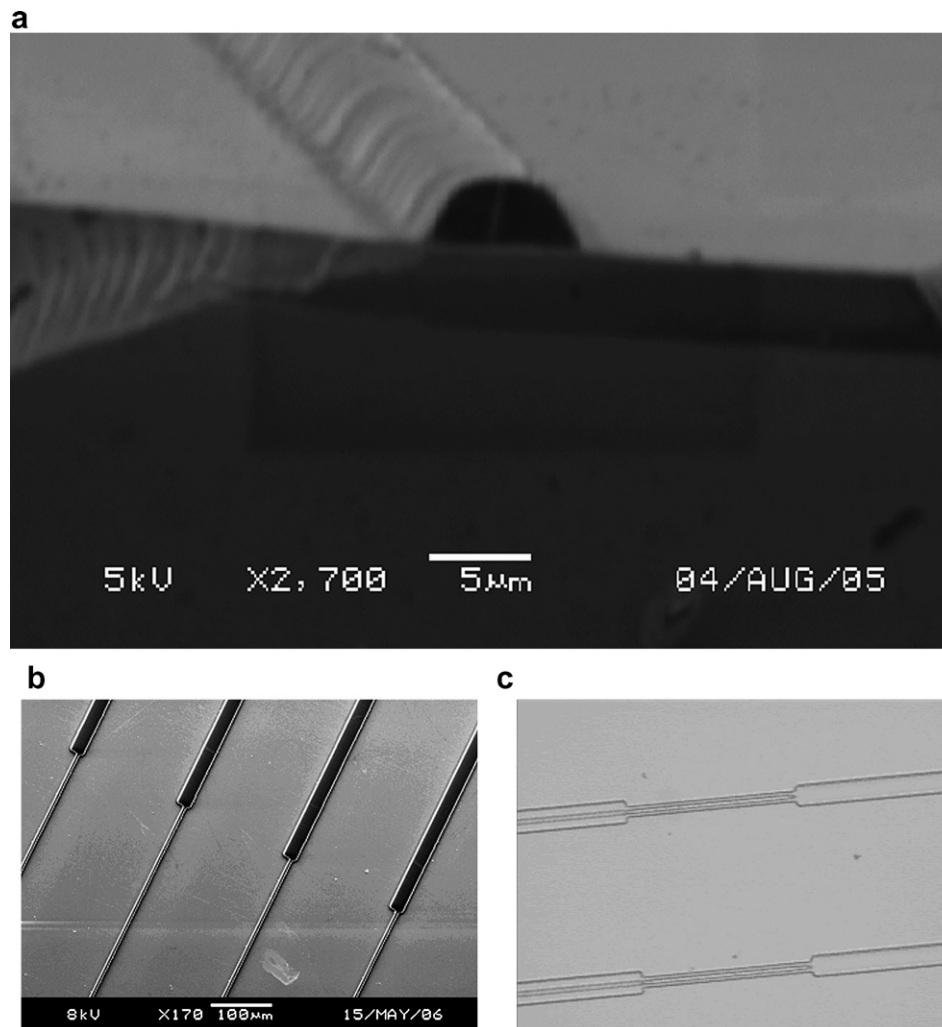

Fig. 5. (a) SEM image of fabricated access waveguides. (b) SEM image of MMI demultiplexer. (c) Microscope image of MMI demultiplexer.

using a germanium (Ge) photodetector and the near field profile is imaged onto an infrared camera integrated with beam analyzer software.

The propagation loss in straight waveguides was measured with the conventional cut-back method. The results, given in Fig. 6, show that the propagation loss of the BCB waveguides is 3.5 dB/cm and the coupling loss is 10.5 dB. The relatively high propagation loss is presumably due to scattering from the sidewall roughness. The high value of coupling loss is mainly due to the size mismatch between the fiber and the waveguide modes.

Images of the output beam for both wavelengths are shown in Fig. 7. The total loss, from the incident power to the output power, was measured to be about 14 dB at both output ports. Of this, 10.5 dB is coupling loss, hence the "insertion loss", defined as the ratio between the power at the output waveguide and that in the input waveguide, is determined to be between 3.2 and 3.5 dB for both output wavelengths (neglecting the small facet reflection loss). This insertion loss comprises the propagation loss through all the MMI as well as the propagation loss through all the straight waveguides. The total length of the straight waveguides is 3.3 mm, hence the propagation loss is estimated to be 1.2 dB for the straight guides and 2.0–2.3 dB for the MMI's. Finally, the crosstalk, defined as the power ratio between the desired wavelength and the unwanted wavelength, was measured to be 14.4 and 20.6 dB for 1310 and 1550 nm, respectively.

For comparison, we note the work of Paiam [8] on the 980/1550 nm demultiplexer based on SiON–SiO$_2$ material system, for which the crosstalk was 18 dB and the insertion loss was 0.5 dB. Although higher insertion loss was recorded in our work we believe that it can be significantly reduced by improving the chemical etching method or by using a dry etching method. The BCB-based CWDM filter
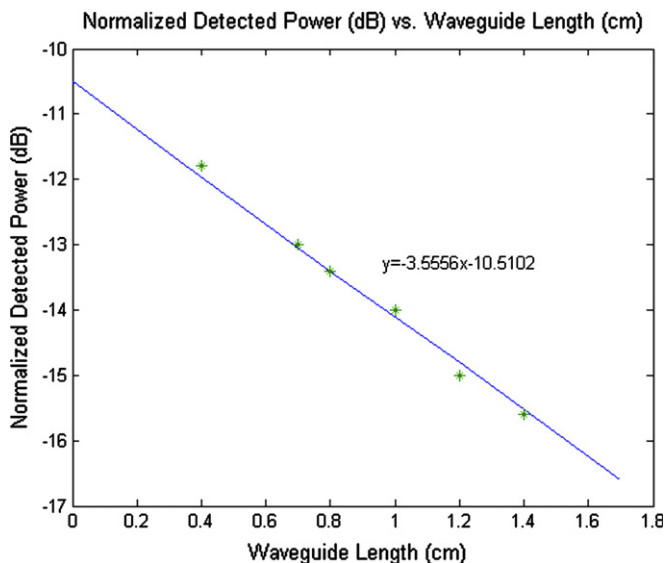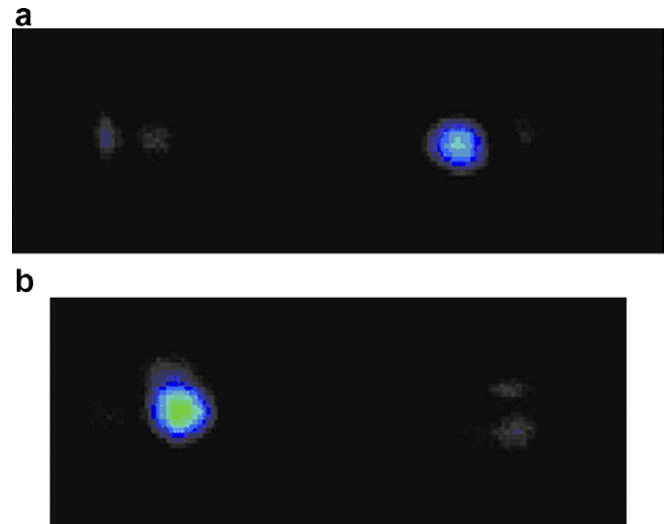

Fig. 7. Near field profile of the demultiplexer outputs: (a) 1310 nm and (b) 1550 nm.

demonstrated in this work will be useful for signal demultiplexing applications due to its significant advantage in reducing the fabrication cost.

5. Conclusion

We have demonstrated an MMI-based CWDM demultipexer for the wavelengths of 1310 and 1550 nm wavelength based on ridge waveguides fabricated in a photodefinable BCB 4024-40 polymer. The structure consists of two cascaded MMI sections, employing general and paired interference mechanism and fabricated on BK7 glass using only chemical etching and standard photolithography. However, due to the quality of the photomask, the resulting sidewall roughness yielded a relatively high waveguide propagation loss of 3.5 dB/cm. Nevertheless, the CWDM demultiplexer is demonstrated to function well with measured crosstalks of 14.4 and 20.6 dB for 1310 and 1550 nm, respectively. The measured insertion loss is around 3.2–3.5 dB for both demultiplexing operations.

Acknowledgments

Fig. 6. Measured output power (normalized by the input power) as a function of waveguide length.

References

[1] H. Kawata, T. Ogawa, N. Yoshimoto, Journal of Lightwave Technology 22 (2004) 1454.
[2] T. Negami, H. Haga, S. Yamamoto, Applied Physics Letters 54 (1989) 1080.

[3] A. Tervonen, P. Poyhonen, S. Honkanen, M. Tahkokorpi, Photonics Technology Letters 3 (1991) 516.

[4] K. Hattori, T. Kitagawa, M. Oguma, Y. Ohmori, M. Horiguchi, Electronics Letters 30 (1994) 856.

[5] P.A. Besse, M. Bachmann, H. Melchior, L.B. Soldano, M.K. Smit, Journal of Lightwave Technology 12 (6) (1994) 1004.

[6] Lucas B. Soldano, E.C.M. Pennings, Journal of Lightwave Technology 13 (4) (1995) 615.

[7] Wei-Ching Chuang, Chih-Yao Chang, Cheng-Chih Lai, Kuen-Cherng Lin, Fiber and Integrated Optics 18 (1999) 93.

[8] M.R. Paiam, C.F. Janz, R.I. MacDonald, J.N. Broughton, Photonics Technology Letters 7 (10) (1995) 1180.

[9] J.M. Heaton, R.M. Jenkins, D.R. Wright, J.T. Parker, J.C.H. Birbeck, K.P. Hilton, Applied Physics Letters 61 (15) (1992) 1754.

[10] F. Wang, J. Yang, L. Chen, X. Jiang, M. Wang, IEEE Photonics Technology Letters 18 (2) (2006) 421.

[11] L. Eldada, L.W. Shacklette, IEEE Journal of Selected Topics in Quantum Electronics 6 (1) (2000) 54.

[12] The Dow Chemical Company. Product Literature: Cyclotene™ Advanced Electronic Resins, May 1999.

[13] K.C. Lin, W.Y. Lee, Electronics Letters 32 (14) (1996) 1259.

[14] S.L. Tsao, H.C. Guo, C.W. Tsai, Optics Communications 232 (2004) 371.

[15] L.B. Soldano, F.B. Veerman, M.K. Smit, B.H. Verbeck, A.H. Dubost, E.C.M. Pennings, Journal of Lightwave Technology 10 (12) (1992) 1843.

[16] W.A. Pasmooij, P.A. Mandersloot, M.K. Smit, Journal of Lightwave Technology 7 (1) (1989) 175.

[17] G.T. Reed, IEE Colloquium on Measurement of Optical Devices (1992) 2/1.

[18] Nourshargh et al., Electronics Letters 21 (18) (1985) 818.

[19] Kassim et al., Single mode rib optical waveguides modelling technique, in: RF and Microwave Conference Proceedings, 2004, p. 272.

[20] N. Dagli, C.G. Fonstad, Applied Physics Letters 46 (6) (1985) 529.